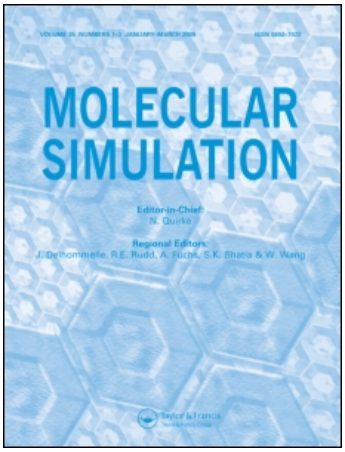

Molecular Simulation
Publication details, including instructions for authors and subscription information:
http://www.informaworld.com/smpp/title~content=t713644482

Stochastic modelling of gradient copolymer chemical composition distribution and sequence length distribution

Andrew S. Cho[a]; Linda J. Broadbelt[a]
[a] Department of Chemical and Biological Engineering, Northwestern University, Evanston, IL, USA

First published on: 22 January 2010

To cite this Article Cho, Andrew S. and Broadbelt, Linda J.(2010) 'Stochastic modelling of gradient copolymer chemical composition distribution and sequence length distribution', Molecular Simulation, 36: 15, 1219 — 1236, First published on: 22 January 2010 (iFirst)
To link to this Article: DOI: 10.1080/08927020903513035
URL: http://dx.doi.org/10.1080/08927020903513035

Molecular Simulation
Vol. 36, No. 15, December 2010, 1219–1236

Taylor & Francis
Taylor & Francis Group

Stochastic modelling of gradient copolymer chemical composition distribution and sequence length distribution

Andrew S. Cho and Linda J. Broadbelt*

Department of Chemical and Biological Engineering, Northwestern University, Evanston, IL 60208, USA

(*Received 1 September 2009; final version received 26 November 2009*)

Stochastic mechanistic models for gradient copolymerisation systems were developed based on a kinetic Monte Carlo algorithm. Due to the discrete nature of the simulations, chains were tracked as binary strings allowing for the storage of the complete sequence of each polymer chain, allowing for an unprecedented level of detail. Models were developed that simulated styrene/4-acetoxystyrene semi-batch gradient copolymer syntheses, and explicit sequence information was determined using simulation results. The chemical composition distribution was mapped for the copolymers, which is capable of providing a visual description of both the size and overall composition distributions of the copolymer and a qualitative description of the chain architecture. This methodology was expanded to track the explicit sequences of each chain that was used to determine the number and weight fraction sequence length distributions. Simulation results show that tail end compositional tapering was never fully achieved. Case studies were conducted to determine the major factors affecting tail end tapering, including increasing the initial batch fraction and varying the 4-acetoxystyrene flow rate. While an increase in initial batch fraction increases 4-acetoxystyrene significantly, head end tapering is lost, while a large increase in flow rate is not capable of fully tapering the tail end.

Keywords: kinetic Monte Carlo; gradient copolymers; chemical composition distribution; sequence length distribution; polymer sequence

1. Introduction

There has been an increasing need for polymeric materials engineered at the microscale for use in highly specialised applications [1]. Polymeric materials that incorporate two or more types of monomers are of particular interest because unique macroscopic properties may result depending on microscopic properties such as composition, degree of polymerisation and arrangement. Alteration of any of these properties can potentially yield materials with significantly different physical properties [2]. Of particular importance is the arrangement, or sequencing, of monomers along each chain. It is possible to have copolymeric materials with similar molecular weight and overall composition, but different arrangements of monomers along each chain, which affects intrachain attractive and repulsive forces and thus macroscopic physical behaviour. An example of this would be random and block copolymers possessing similar compositions and size but significantly different chain sequencing; while a random block copolymer would exhibit a single glass transition temperature with a value that is between those of its two component polymers, a block copolymer possesses two glass transition temperatures corresponding to its respective polymer blocks. Therefore, it is of key importance not only to measure the size and composition of these materials, but also to determine the relative arrangement of monomers along each chain.

A particular family of copolymeric materials that have gained significant attention for their unique properties is gradient copolymers [3,4]. These materials are intermediate between random and block copolymers, possessing a smooth composition gradient along each chain. Due to the unconventional dispersion of intrachain attractive and repulsive forces, gradient copolymers possess physical properties unique to their respective random and block copolymer counterparts. One particular application for which gradient copolymers have shown much potential is in the field of blend compatibilisation [5–7]. While block copolymers have been used in compatibilisation applications, above a critical micelle concentration (CMC), they tend to undergo self-assembly and aggregate at the blend interface, providing little adhesion effects. Gradient copolymers possess a higher CMC due to the dispersion of intrachain repulsive forces along the chain, and experimental studies have confirmed that these materials show significantly stronger adhesion effects compared to their block copolymer counterparts. Additionally, more recent work has examined the unique mechanical properties of gradient copolymers and their potential use in damping applications [8,9].

*Corresponding author. Email: broadbelt@northwestern.edu

ISSN 0892-7022 print/ISSN 1029-0435 online

DOI: 10.1080/08927020903513035
http://www.informaworld.com

Synthesis of these materials requires a controlled method of polymerisation in order to control monomer arrangement and molecular weight while maintaining chain lengths. While anionic methods have shown the ability to synthesise gradient copolymers, they are better described as tapered block copolymers [10]. Additionally, the choice of comonomers is limited, and synthesis is highly susceptible to contamination. More robust methods of synthesising gradient copolymers involve the use of controlled radical polymerisation (CRP), which is capable of controlling chain architecture while maintaining a low polydispersity. CRP benefits from the presence of a stable transient radical species which is capable of reversibly attaching to propagating radical chains. Because this essentially eliminates biradical termination which is responsible for high polydispersities and lack of control, polymerisation proceeds in a manner similar to true controlled methods.

Gradient copolymers have successfully been synthesised using various methods of CRP, including atom transfer radical polymerisation [11] and reverse addition–fragmentation transfer polymerisation [12]. One particular method of CRP that has shown to be successful in the synthesis of styrenic gradient copolymers is nitroxide-mediated (NM) CRP [7,13,14], in which a stable nitroxide radical is used as a transient radical species. Since chains are allowed to propagate at a more uniform rate, this allows for the synthesis of materials with low polydispersities and control over molecular weights. Although it is possible to create materials with spontaneous composition gradients along each chain using CRP, semi-batch synthesis is the predominant methodology utilised in gradient copolymerisation. Compared to batch methods, semi-batch synthesis provides control over the steepness of the chainwise composition gradient. In these methods, one monomer is added during the course of polymerisation, which allows for relative control of the chainwise sequencing through the flow rate of the added monomer, enabling one to tailor the shape of the composition gradient [15].

Although experimental studies have been successful in the creation and characterisation of gradient copolymers, analysis of these materials has only been performed at a macroscopic level, as experimental methods are generally limited to determination of molecular weight averages and overall compositions. More quantitative experimental methods to describe chain sequence, including the explicit sequence length distribution (SLD) of copolymers, do not exist. The approaches that are the closest to uncovering the explicit SLD are measurement of the distribution of monomer triads via NMR [16] and, more recently, investigations based on the Kerr effect [17,18]. A small number of modelling studies have been carried out as reported in the literature which have attempted to describe the explicit SLD of copolymers in a compacted format through the encoding of individual chains [19–21]. However, this methodology is limited to short chain lengths, and the decimal encoding of sequence, while explicit, is not easily digested. More recently, Monte Carlo models have been developed by others based on Markov chains able to track triad distributions and average sequence lengths for batch copolymerisation cases [22]. However, we sought to employ a more comprehensive mechanistic modelling scheme based on a semi-batch process to examine compositional distributions, and we explicitly tracked the monomer-by-monomer sequence of every chain so that a full range of statistics about sequence could be extracted.

Recent studies in the literature have focused on the description of the copolymer chemical composition distribution (CCD), which provides information regarding the size distribution as well as the relative monomer arrangement of a copolymer, as a means of providing insight into these systems. The CCD of a copolymer provides a bivariate distribution of the number of chains with a particular composition and size. Based on the shape of this distribution, the relative chain architecture can be inferred, which facilitates the differentiation of various copolymeric architectures, such as random, alternating and blocky morphologies. Additionally, the CCD of a copolymer can readily be compared to experimental results produced from MALDI-ToF-MS, which has been shown to successfully provide the CCD, or a unique copolymer 'fingerprint', of these materials [23–25].

The first approach to specifying the CCD of a copolymeric material was developed by Stockmayer [26], who provided an analytical expression to describe the weight distribution as a function of kinetic chain length and composition. Similar approaches have yielded modifications to the Stockmayer equation to account for monomer molar masses [27] as well as statistical approaches to provide similar bivariate distributions [28]. More recent studies have utilised Monte Carlo modelling in the analysis of ethylene copolymer composition distributions [28,29]. Although these models are successful in producing composition distributions, they are not based on actual polymerisation reaction systems. To date, there has yet to be a study involving the incorporation of the CCD within a comprehensive kinetic modelling framework. In our previous research, we developed kinetic modelling tools using a mechanistic framework which is capable of predicting key features of polymerisation systems including concentrations of different species and molecular weight evolution [30,31]. Expanding this methodology to explicitly track chains at the molecular level allows for a more explicit description of a copolymer system, capable of providing not only the size distribution but the CCD as well. Utilising kinetic Monte Carlo (KMC), chain size and composition distributions can be generated allowing for direct comparison to experimental results.

For this study, a styrene/4-acetoxystyrene NM-CRP copolymerisation system using α-methyl-styryl-di-*tert*-butyl nitroxide (referred to as A-T) as a unimolecular alkoxyamine initiator was examined. The A-T alkoxyamine has been shown to be successful in the controlled polymerisation of styrene [32,33] and 4-acetoxystyrene as shown in previous work [34]. Experimental studies have successfully utilised A-T in semi-batch syntheses to produce styrene/4-acetoxystyrene gradient copolymers [7,14,35]. 4-Acetoxystyrene, while not as commonly utilised as styrene, has been examined in studies for its use as a precursor in the synthesis of 4-hydroxystyrene which has use as a photoresist material [36,37]. Recent modelling studies involving the NM-CRP of 4-acetoxystyrene have been discussed in our previous work [31,34]. While both monomers lead to important homopolymers, their copolymers are equally interesting, since styrene/4-hydroxystyrene gradient copolymers, which are created from styrene/4-acetoxystyrene gradient copolymers, have been shown to be effective in blend compatibilisation [7] as well as possessing unique physical properties [8]. Kinetic rate parameters for the respective homopolymer systems were previously determined for these systems using a combined experimental and modelling approach in our laboratory [30,31].

Using the experimental set-up of Kim et al. [7] as a basis for our models, our stochastic modelling framework was able to capture key features of gradient copolymerisation systems. In this work, we sought to utilise our modelling methodologies to provide composition and sequence distribution data to provide a more detailed description of the products of NM-CRP gradient copolymerisation. Explicit modelling of these products allows for a quantitative characterisation of gradient copolymer composition and sequence at a microscopic level.

2. Model development

2.1 Mechanistic chemistry

Using Mayo–Lewis terminal model kinetics, copolymerisation behaviour is defined by the reactivity ratios of the monomer pair, $r_1 = k_{11}/k_{12}$ and $r_2 = k_{22}/k_{21}$, where k_{ii} represents the self-propagation rate constant of monomer i and k_{ij} is the cross-propagation rate constant for monomer j adding to a growing chain with monomer i as the terminal unit [38]. The monomer pair of styrene and 4-acetoxystyrene has similar cross-reactivities as indicated by their reactivity ratios in bulk polymerisation, with $r_1 = 0.86$ and $r_2 = 1.26$ [39]. This indicates that these monomers have a slight bias towards 4-acetoxystyrene propagation, although this difference is responsible for only a slight compositional drift. Because 4-acetoxystyrene is a styrenic monomer, a large polarity difference between the two monomers does not exist and thus 4-acetoxystyrene and styrene have similar reactivities. This facilitates control over the chainwise composition as a semi-batch method can be used to tailor the architecture during the course of the polymerisation. Additionally, the product of the reactivity ratios equals unity, which adheres to the ideal copolymerisation case in which no significant penultimate effect is expected [40,41]. For these reasons, the Mayo–Lewis terminal model was assumed to be valid

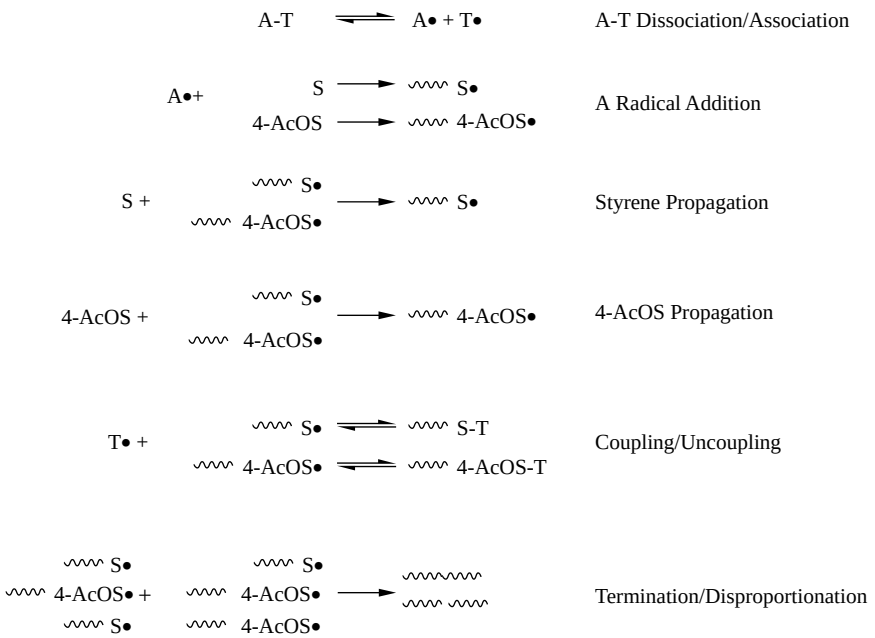

Figure 1. Base reactions used in NM-CRP copolymerisation model.

in describing the cross-propagation kinetics for our copolymerisation model.

The reactions included in the NM-CRP mechanism were based on previous modelling work in our laboratory [30,31] and included homopolymerisation reactions as well as copolymerisation reactions based on terminal model kinetics. The base reactions included within our modelling framework are shown in Figure 1: initiator dissociation and association with nitroxide, initiator radical addition, propagation reactions, nitroxide coupling and uncoupling, and termination by recombination and disproportionation. For propagation and termination, appropriate cross-reactions were included as shown for reactions between opposite monomer pairs.

Using a mechanistic framework, it was determined in our previous work [30] with styrene NM-CRP that two key side reactions compromised the living behaviour of the system: thermal polymerisation and chain transfer to monomer. Thermal initiation is responsible for the continuous production of radicals during the course of a polymerisation. Although chain transfer to monomer was shown to have a minor effect on the molecular weight averages obtained in NM-CRP at lower temperatures [30], it is generally regarded as a fundamental reaction within the free radical polymerisation framework and therefore was included. These reactions were included with the base reactions to form a similar mechanism as that used to model styrene NM-CRP. These reactions are shown in Figure 2: thermal initiation involving like and opposite monomers, thermal radical addition, chain transfer to monomer and monomeric radical addition. For thermal initiation, it was assumed that the radicals formed were identical to those of the reacting monomer; for cross-initiation, it was assumed that one of each type of radical was produced. The monomeric radicals generated by chain transfer to monomer were identical to the reacting monomer.

2.2 Kinetic Monte Carlo

KMC models were developed based on the exact stochastic simulation algorithm developed by Gillespie [42,43]. Rather than using macroscopic species concentrations as with continuum-based models, these models are explicit in that they are based on the number of molecules within a microscopic-scaled homogeneous reaction volume representative of the complete system. Because reaction rates in KMC are represented discretely, reaction rates must be converted from macroscopic values on a per volume basis to stochastic rates based on the total number of molecules within the scaled reaction volume. Using a suitable scaled volume, species' concentration must be converted to a discrete number of molecules based on macroscopic values. Additionally, rate coefficients must be converted from a per volume basis to an event basis:

$$k^{\mathrm{MC}} = k^{\mathrm{cont}}, \quad \text{first-order reactions,}$$

$$k^{\mathrm{MC}} = \frac{k^{\mathrm{cont}}}{VN_{\mathrm{A}}}, \quad \text{second-order reactions between different species,}$$

$$k^{\mathrm{MC}} = \frac{2k^{\mathrm{cont}}}{VN_{\mathrm{A}}}, \quad \text{second-order reactions between same species,}$$

$$k^{\mathrm{MC}} = \frac{6k^{\mathrm{cont}}}{(VN_{\mathrm{A}})^2}, \quad \text{third-order reactions between same species,}$$

where k^{MC} represents a Monte Carlo rate coefficient; k^{cont}, a continuum rate coefficient; V, the scaled volume and N_{A}, Avogadro's number.

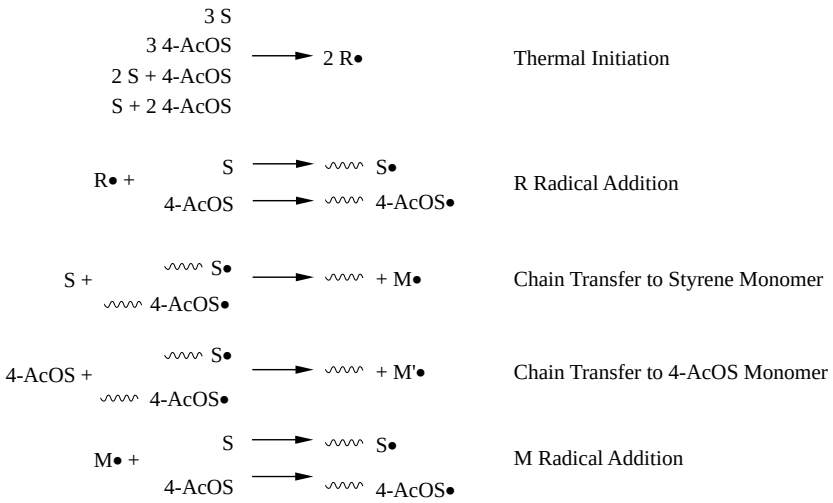

Figure 2. Side reactions included in NM-CRP copolymerisation model.

The reaction channels shown in Figures 1 and 2 occur on a microscopic basis and occur stochastically based on reaction probabilities:

$$\sum_{\nu=1}^{\mu-1} P_\nu < r_1 < \sum_{\nu=1}^{\mu} P_\nu, \tag{1}$$

where μ is the index of the selected reaction channel; P_ν, the probability of the νth reaction channel and r_1, a random number uniformly distributed between 0 and 1. Probabilities for each reaction are determined based on its fraction of the total rate of reaction:

$$P_\nu = \frac{R_\nu}{\sum_{\nu=1}^{M} R_\nu}, \tag{2}$$

where R_ν is the stochastic rate of the νth reaction and M is the total number of reaction channels. The time interval between reactions is determined by

$$\tau = \frac{1}{\sum_{\nu=1}^{M} R_\nu} \ln\left(\frac{1}{r_2}\right), \tag{3}$$

where r_2 is another random number uniformly distributed between 0 and 1.

Using the stochastic rate equations, the model is solved using an iterative procedure. The simulation process is outlined in the flow chart shown in Figure 3. Initial variables for reactant concentrations and reaction conditions are set at the onset of the simulation. During each iteration, stochastic rates are calculated and two random numbers are generated, one used to determine the particular reaction channel probabilistically using Equation (1) and the other to establish a reaction time using Equation (3). Following selection of a reaction channel, reacting species are updated based on the occurrence of the reaction and distribution data are also updated.

Although KMC models are significantly more computationally intensive compared to continuum-based models such as the method of moments, due to the discretisation of individual molecules, they are capable of providing a higher level of detail of the system, including the full molecular weight distribution (MWD), copolymer CCD and SLD. The copolymer CCD plots can be used as fingerprints of copolymer topologies and compared to experimental results produced by MALDI-ToF-MS. In order to keep track of the copolymer CCD, composition and thus size, data for each chain species, including live radicals, capped dormant radicals and dead polymer (DP), were stored during the course of the simulation.

The styrene/4-acetoxystyrene semi-batch gradient copolymerisation data produced by Kim et al. [7] were used as a basis of comparison for our KMC models. In this polymerisation, an alkoxyamine macroinitiator was used as a source of initiating radicals and nitroxide radicals, similar to the A-T alkoxyamine used in previous studies. The macroinitiator consisted of a short segment of styrene ($M_n \sim 8400$ g/mol) capped with di-*tert*-butyl-nitroxide. The initial reaction mixture for this synthesis consisted of styrene and the macroinitiator at a concentration of 1.31×10^{-3} mol/l and the temperature was 90°C. 4-Acetoxystyrene was added at a rate of 0.05 ml/min over the course of the 4 h polymerisation. Aliquots were removed during the course of polymerisation, with molecular weight averages estimated using GPC-LS and compositions measured using NMR, allowing the comparison of compositional change vs. normalised chain length.

Kinetic parameters used in the model were taken from previous studies involving styrene and 4-acetoxystyrene homopolymerisation [30,31]. Cross-propagation rate constants were determined using reactivity ratios, $r_1 = 0.86$ and $r_2 = 1.26$, obtained from the literature for bulk polymerisation [39], while parameters for cross-thermal initiation and cross-termination were approximated using an algebraic mean of homopolymerisation values for activation energies and a geometric mean for frequency factors. The parameters used in the model are shown in Table 1. Simulations used an increased value of 2×10^{11} initial molecules compared to earlier hompolymerisation studies [34] to increase resolution demanded by the presence of two unlike monomers.

3. Results and discussion

3.1 KMC gradient copolymerisation CCD

A comparison of the cumulative copolymer composition as denoted by the fraction of styrene monomer measured experimentally and the model predictions is shown in Figure 4. These results indicate that the kinetic parameters are able to capture the experimental data reasonably well. However, the KMC model has the ability to track the composition of individual chains, so we sought to further expand the analysis of the chain architecture through examination of the CCD produced by the model. The CCD for the simulated gradient copolymerisation of styrene/4-acetoxystyrene using the experimental conditions of Kim et al. is shown in Figure 5. Of particular significance are the discrete lobes in the plot, which are very distinct compared to ideal cases in a batch reactor presented for other systems [23,44,45]. In those simulations, the simulated CCD plots were continuous plots emanating from the origin, as there was no macroinitiator involved and all chains were initiated by radicals. It is evident in the CCD for the semi-batch, macroinitiated polymerisation that distinct regions exist corresponding to: (1) polymer initiated by the macroinitiator, which is represented by the larger, high molecular weight lobe and (2) polymer initiated by radicals that are continuously produced by thermal initiation and chain transfer to monomer, which is represented by the lobe emanating from the origin. In order to confirm the origins of these lobes, the model was

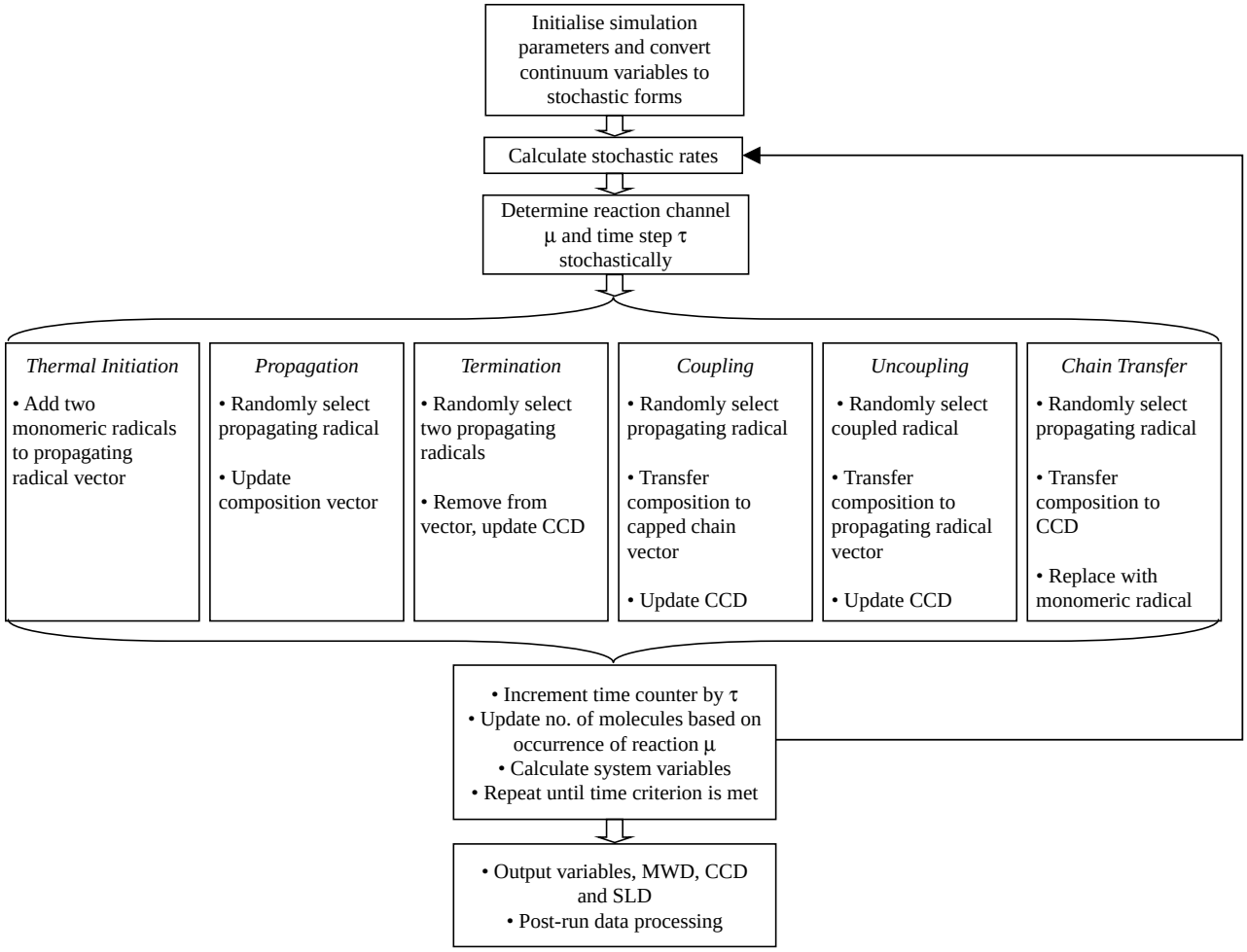

Figure 3. KMC model flow chart.

modified to report the CCD for distinct types of chains: macroinitiated capped polymer (A-T), capped polymer initiated by continuously generated radicals from thermal initiation and chain transfer to monomer (R/M-T) and DP at various times during the polymerisation. The individual CCD plots for these chain types for polymerisation times of 1–4 h are shown in Figures 6–9, respectively.

Early on in the polymerisation, the chain fractions have similar average compositions as indicated by their slopes. The R/M-T fraction consists mostly of short-capped chains, while the DP is composed of macro-initiated chains that have undergone termination with other macroinitiated chains as well as R/M-initiated chains, leading to the presence of two distinct lobes. Over the course of the polymerisation, the effect of the compositional drift is evident in the macroinitiated capped chains as shown in Figures 6–9. The slope of the centre line of the lobe decreases over time, indicating increasing amounts of 4-acetoxystyrene incorporation into these chains. The curvature of this lobe is indicative of this as well; shorter chains possess a higher fraction of styrene compared to longer chains which have undergone propagation with increasing batch fractions of 4-acetoxystyrene. It is also interesting to note that the change in the slope of the other two types of chains is different compared to the capped macroinitiated chains. The slope of the R/M-T lobe decreases more significantly compared to the A-T fraction, approaching a value close to unity. Additionally, the curvature of this lobe is opposite of the macroinitiated chains; shorter chains possess a lower fraction of styrene compared to chains with higher degrees of polymerisation. These chains are continuously initiated during the course of the polymerisation and do not propagate to a significant extent as evidenced by the fact that the majority of these chains are concentrated at lower degrees of polymerisation. Therefore, these chains have a similar composition to the reactor composition, which approaches equimolarity towards the end of the polymerisation. However, there is a small portion of these chains that has undergone a significant amount of

Table 1. Kinetic parameters used in styrene/4-acetoxystyrene (AcOS) copolymerisation model.

Reaction	Frequency factor, A (s^{-1}, $l\,mol^{-1}\,s^{-1}$ or $l^2\,mol^{-2}\,s^{-1}$)	Activation energy, E_a ($kJ\,mol^{-1}$)
Initiator uncoupling	3.8×10^{14}[a]	120.0[a]
Initiator coupling	1.65×10^{10}[b]	6.3[c]
Initiator radical addition to styrene	4.27×10^{7}[d]	32.5[d]
Initiator radical addition to 4-AcOS	4.97×10^{7}[e]	32.5[d]
Styrene thermal initiation	6.3×10^{5}[f]	114.9[f]
4-AcOS thermal initiation	1.35×10^{3}[g]	97.1[h]
Cross-thermal initiation	2.92×10^{4}[i]	106.0[j]
Styrene homopropagation	4.27×10^{7}[d]	32.5[d]
4-AcOS homopropagation	1.79×10^{7}[g]	28.7[g]
Styrene/4-AcOS cross-propagation	4.97×10^{7}[e]	32.5[d]
4-AcOS/styrene cross-propagation	1.42×10^{7}[k]	28.7[g]
Styrene nitroxide uncoupling	3.8×10^{14}[a]	120.0[a]
Styrene nitroxide coupling	1.65×10^{10}[b]	6.3[c]
4-AcOS nitroxide uncoupling	3.8×10^{14}[a]	123.8[h]
4-AcOS nitroxide coupling	1.65×10^{10}[l]	6.3[c]
Chain transfer to monomer (all)	2.31×10^{6}[m]	53.0[m]
Styrene recombination	2.45×10^{9}[n]	6.3[c]
Styrene disproportionation	4.31×10^{8}[n]	6.3[c]
4-AcOS recombination	1.07×10^{10}[h]	6.3[c]
4-AcOS disproportionation	1.88×10^{9}[h]	6.3[c]
Cross-recombination	5.12×10^{9}[i]	6.3[j]
Cross-disproportionation	9.00×10^{8}[i]	6.3[j]

[a] Styrene uncoupling parameter for di-*tert*-butyl-nitroxide [47]. [b] Frequency factor backed out using an equilibrium constant $K \sim 10^{-12}$ M [48]. [c] Determined for styrene biradical termination at ambient pressure [49]. [d] IUPAC k_p for styrene [50]. [e] Determined using styrene IUPAC k_p [50] with $r_1 = 0.86$ for styrene/4-acetoxystyrene cross-propagation in the bulk [39]. [f] Determined by Campbell et al. [51] for styrene. [g] Determined in 4-acetoxystyrene thermal polymerisation study of Li et al. [31]. [h] Fitted in 4-acetoxystyrene NM-CRP study in previous work assuming 85% recombination and 15% disproportionation. [i] Geometric mean of styrene and 4-acetoxystyrene frequency factors. [j] Algebraic mean of styrene and 4-acetoxystyrene activation energies. [k] Determined using 4-acetoxystyrene k_p with $r_2 = 1.26$ for 4-acetoxystyrene/styrene cross-propagation in the bulk [39]. [l] Frequency factor used for styrene/di-*tert*-butyl-nitroxide uncoupling. [m] Determined by Hui and Hamielec [52] for styrene. [n] Fitted in styrene NM-CRP study in previous work assuming 85% recombination and 15% disproportionation.

propagation as evidenced by the increase in the slope at higher degrees of polymerisation; the slope approaches that of the A-T fraction as these chains have undergone significant propagation at higher batch fractions of styrene.

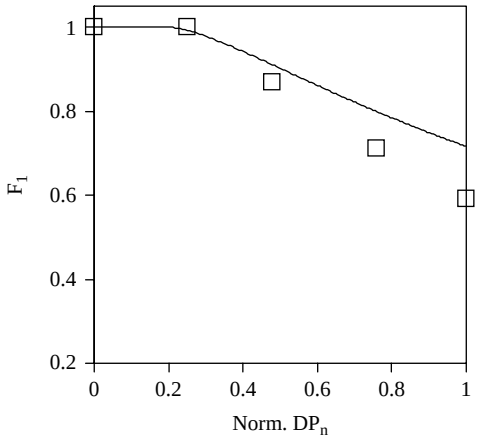

Figure 4. Cumulative fraction of styrene (monomer 1) in the copolymer vs. normalised chain length (degree of polymerisation at a given reaction time divided by the degree of polymerisation at the final reaction time) for styrene/4-AcOS macroinitiated gradient copolymer. Simulation results shown as the line with open symbols denoting experimental data obtained by Kim et al. [7].

Compared to the other lobes, the DP fraction undergoes little change; while DP chains have an increasing fraction of 4-acetoxystyrene, they are not present in high number.

The KMC model is capable of providing the full MWD of the polymerisation including revealing the MWD of different chain fractions. For this copolymerisation study, rather than utilising the MWD, the number

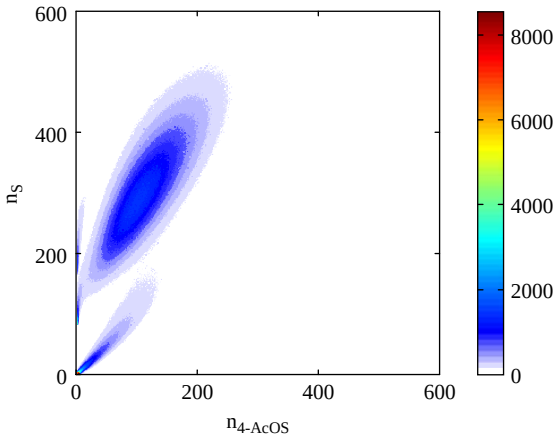

Figure 5. CCD for styrene/4-AcOS macroinitiated gradient copolymer at 4 h.

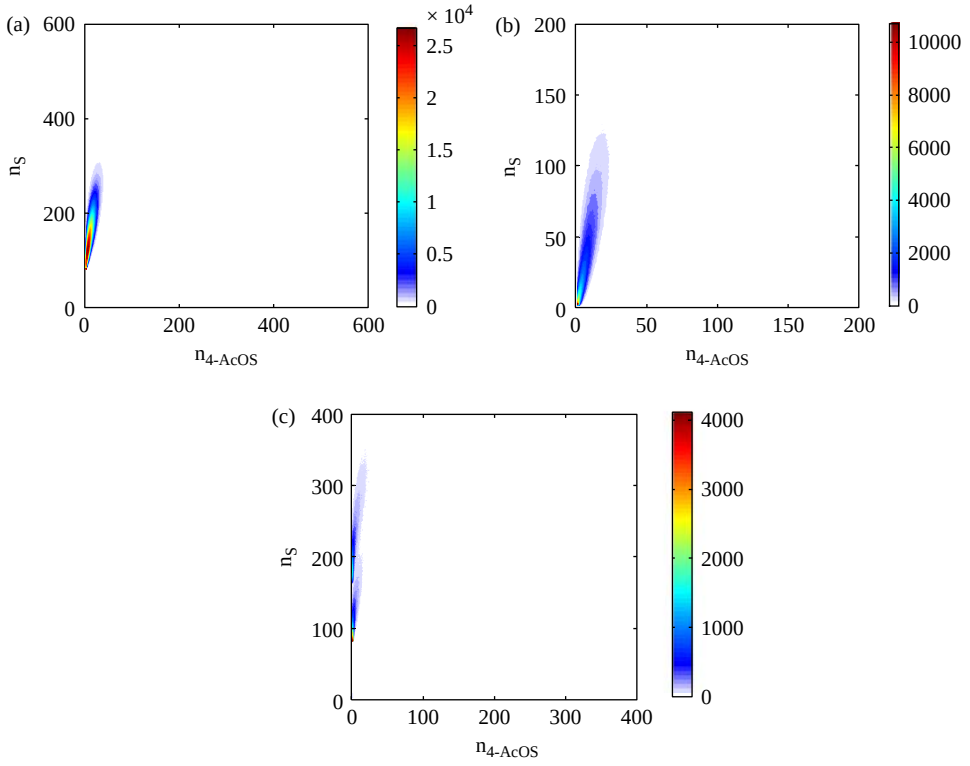

Figure 6. CCD plots for macroinitiated gradient copolymer after 1 h of polymerisation for (a) macroinitiated chains, (b) R/M-initiated chains and (c) DP.

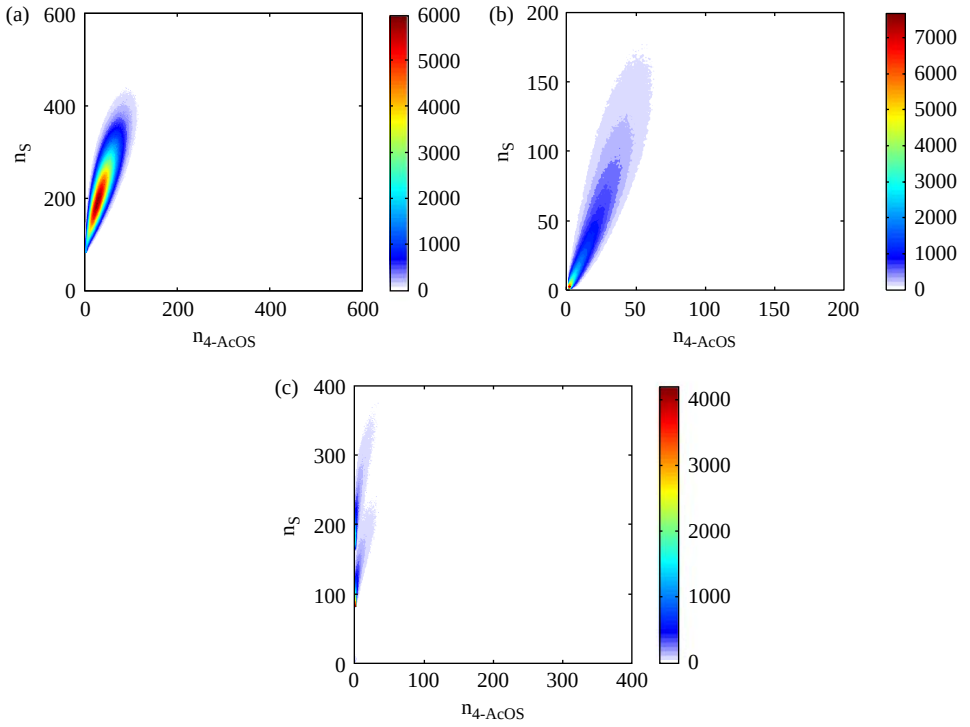

Figure 7. CCD plots for macroinitiated gradient copolymer after 2 h of polymerisation for (a) macroinitiated chains, (b) R/M-initiated chains and (c) DP.

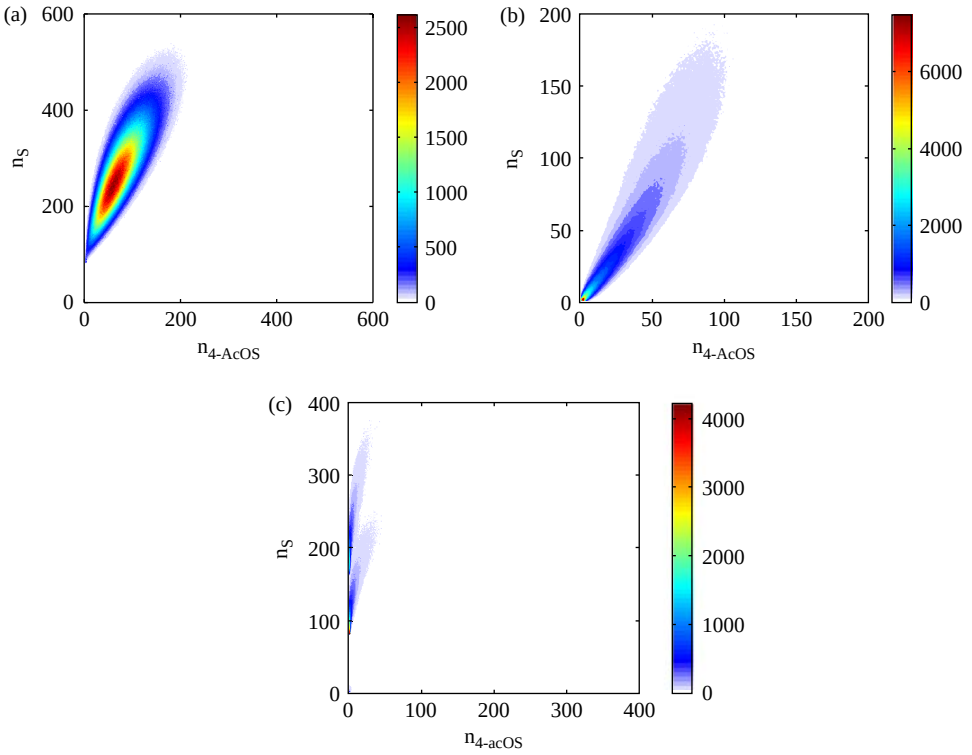

Figure 8. CCD plots for macroinitiated gradient copolymer after 3 h of polymerisation for (a) macroinitiated chains, (b) R/M-initiated chains and (c) DP.

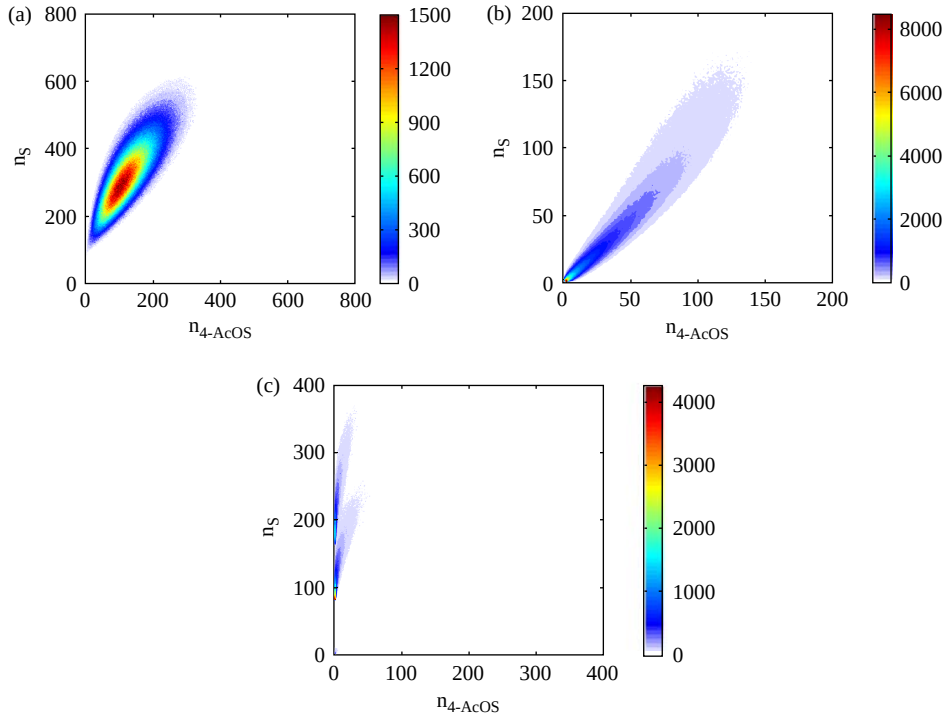

Figure 9. CCD plots for macroinitiated gradient copolymer after 4 h of polymerisation for (a) macroinitiated chains, (b) R/M-initiated chains and (c) DP.

average degree of polymerisation distribution was used since composition was not uniform between chain fractions, with the A-T, R/M-T and DP chain fractions containing 72, 57 and 81% styrene, respectively, at the conclusion of polymerisation. Using the model, the individual size distribution of each chain type was generated at the end of polymerisation. Figure 10 displays the number average degree of polymerisation distribution for macroinitiated capped chains, capped chains initiated by thermal and monomeric radicals and DP. It is apparent from the plot that macroinitiated capped chains constitute the largest fraction of chains (76%) as well as being the longest in the system (DP_n of 462), indicating a high degree of livingness. Capped chains initiated by thermal and monomeric radicals and DP comprise a smaller fraction of the chains in the system at 14 and 10% with average chain lengths of 222 and 433, respectively.

The use of KMC provides a high level of detail of gradient copolymerisation systems compared to continuum-based models that have been developed previously, as it allows for the creation of explicit size distributions as well as the copolymer fingerprint, or CCD. The CCD provides an excellent means of ascertaining the general features of monomer arrangement of a copolymer. However, it is still not an explicit measure of the SLD, which aims to describe exactly how monomers are arranged along the backbone.

3.2 KMC gradient copolymerisation triad distribution

The results of the KMC simulations described to this point offer significant insight into the sequence characteristics of copolymers. However, we sought to provide a more quantitative description of the sequence characteristics of these systems. In order to accomplish this, the KMC framework was expanded to track the explicit sequence of individual chains so that statistics regarding the sequence length and triad distributions could be extracted. Instead of storing overall composition information for each chain, the vectors used in KMC were altered to keep track of chains as binary strings representing individual chain sequences, where a 0 was used to represent styrene and a 1 was used to denote 4-acetoxystyrene. PERL scripts were then used to quantify triad and SLDs from raw simulation output. Although this was significantly more computationally intensive than tracking just the overall composition of each chain, the explicit tracking of individual chains provides an unprecedented level of detail which has not been realised within the framework of a detailed mechanistic model to date.

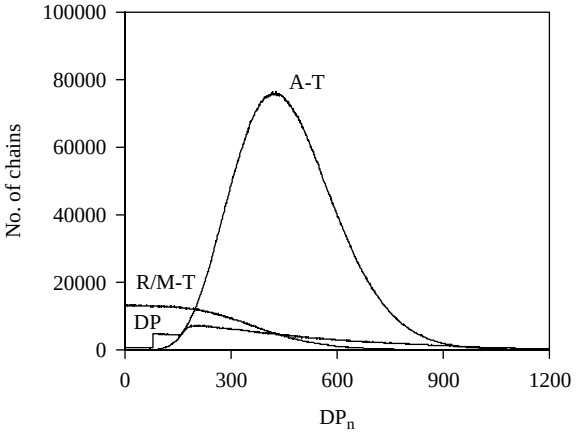

Figure 10. Number average degree of polymerisation distribution for different chain fractions of macroinitiated gradient copolymer.

Our initial analysis calculated the triad distribution of the eight possible triads for the three different chain fractions: capped radicals initiated by thermal and monomeric radicals, capped radicals initiated by the macroinitiator and dead chains. The triad distributions for each chain type at various times are shown in Figure 11. For convenience, triads are labelled as binary strings, with 0 representing styrene and 1 representing 4-acetoxystyrene. As expected, the 000 triad is the dominant sequence early in the polymerisation as shown in the 1 h distribution; each of the three chain types is dominated by styrene monomer as both the macroinitiator and initial monomer charge consisted entirely of styrene. Triad sequences including two styrene units were the next most abundant, and sequences involving two or more 4-acetoxystyrene units were the smallest fractions. Over the course of the polymerisation, increasing amounts of 4-acetoxystyrene were incorporated into the polymer as evidenced by the increase of triads including one or more 4-acetoxystyrene units.

Relative to the other chain types, the DP fraction contains the highest fraction of 000 triads throughout the course of the reaction, indicating that this portion contains predominantly macroinitiated chains which have undergone little propagation, consistent with the DP CCD in Figure 9(c). The DP chain fraction shows the least amount of incorporation of the 4-acetoxystyrene monomer, indicating that, throughout the polymerisation, DP predominantly consists of long sequences ($DP_n = 433$) of predominantly styrene (81%) which comprise the smallest fraction of chains at 10%. Conversely, the capped chains initiated by thermal and monomeric radicals show the lowest fraction of 000 triads throughout the reaction. This is to be expected as this is the only chain fraction that does not contain chains that were initiated by the macroinitiator. Instead, these chains are continually initiated over the course of the polymerisation and their composition should most closely match that of the reaction mixture. Over the course of the polymerisation, this portion continually shows the highest fraction of

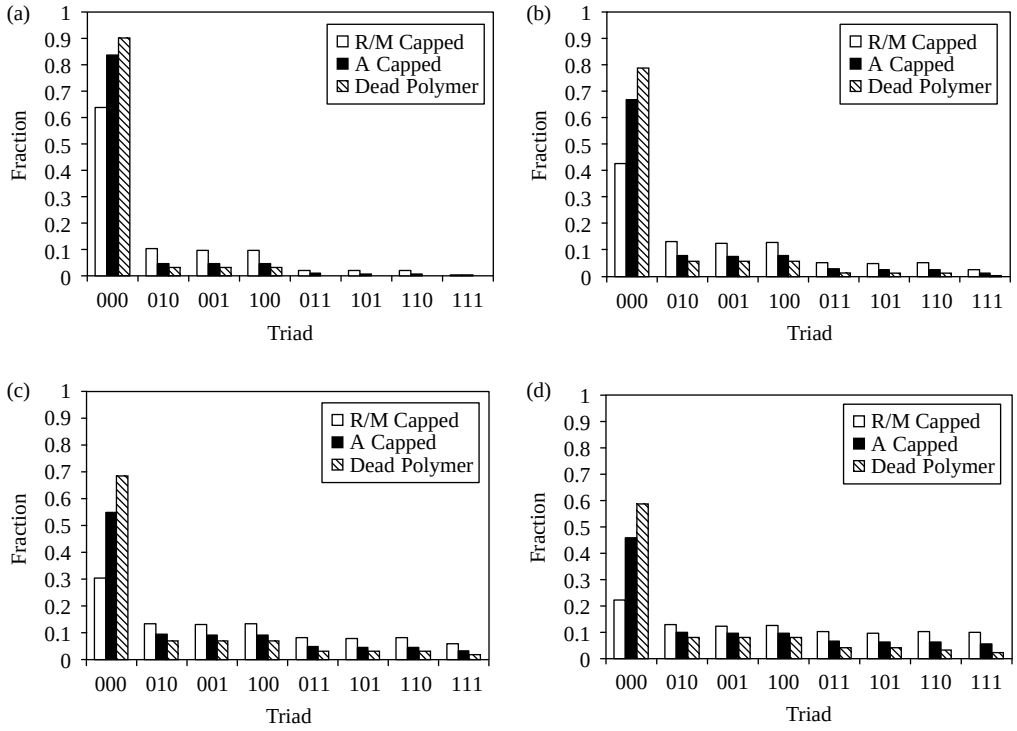

Figure 11. Triad distribution for chain fractions of macroinitiated gradient copolymer at times of (a) 1 h, (b) 2 h, (c) 3 h and (d) 4 h. 0 is used to represent styrene and 1 is used to denote 4-acetoxystyrene.

4-acetoxystyrene-rich containing fractions. As shown by the CCD in Figure 9(b), these are predominantly shorter chains ($DP_n = 222$) with the lowest fraction of styrene among the different chain fractions (57%) and comprise 14% of the total chains in the system. A similar decrease in the 000 triad is seen in the macroinitiated capped radicals, as they increasingly incorporate more 4-acetoxystyrene as the batch charge approaches an equimolar composition. However, this fraction consists of longer chains ($DP_n = 462$) with a significantly larger fraction of styrene (72%) which account for the majority of the chains in the system at 76%.

It is evident from the triad distributions that 4-acetoxystyrene does not get incorporated to a significant extent, as the final triad distribution shows a predominance of styrene within the copolymer with a final styrene mole fraction of 0.72. Although the capped chains initiated by thermal and monomeric radicals exhibit a reasonable amount of incorporation, the macroinitiated fraction, which represents the majority of the gradient copolymer, contains a significant fraction of styrene at the conclusion of the polymerisation. At the end of the polymerisation, the 000 triad is still the dominant fraction while there is not a significant increase in the fraction of 4-acetoxystyrene-rich triads, indicating that 4-acetoxystyrene is not heavily incorporated at the tail end of the chains.

3.3 KMC gradient copolymerisation SLD

Using the same simulation output, PERL scripts were utilised to determine the SLDs for the three chain types by collecting the number of homologous monomer segments of varying lengths. Commonly, the SLD is summarised through the calculation of the number and weight average sequence length, n_A and w_A, respectively:

$$n_A = \frac{\sum_i iN_i}{\sum_i N_i}, \tag{4}$$

$$w_A = \frac{\sum_i i^2 N_i}{\sum_i iN_i}, \tag{5}$$

where i represents the sequence length and N_i is the number of homologous sequences of monomer A of length i [16]. By definition, the number average sequence length gives a relative idea of the chain morphology; larger values indicate long segregated segments of a particular monomer which can be inferred as blockiness while smaller values indicate a higher degree of alternation. The weight average sequence length provides analogous information with weighting based on sequence length rather than number. Similar to molecular weight averages, the uniformity of sequence lengths can be described using

a dispersity index, which we term SDI:

$$\mathrm{SDI} = \frac{w_A}{n_A}. \tag{6}$$

Therefore, comparison of the average sequence lengths should provide another estimate of the level of incorporation of each comonomer during the course of the polymerisation as well as the dispersity of the SLD. Note that our related work [46] has shown that the classic theory describing the distribution of instantaneous segment lengths developed for conventional free radical polymerisation does not always hold in CRP. Segment formation can be controlled by deactivation through coupling of growing radicals and nitroxide radicals instead of selective preference during propagation due to different reactivity ratios and composition of competing monomers if the transient lifetime is too short. Thus, depending on the reaction conditions, classic equations based on composition and reactivity ratios only fail to describe the sequence lengths.

The average sequence lengths and SDI for styrene and 4-acetoxystyrene are shown in Figure 12(a) and (b), respectively. Over the course of the reaction, the number and weight average sequence lengths for styrene undergo a significant decrease (15.85–4.4 and 70.21–37.6 for number and weight averages, respectively) accompanied by an increase in SDI (4.5–8.55). These sequence averages undergo a significant decrease due to the presence of the macroinitiator while the SDI increases due to a broadening of the sequence distribution as shown in Figure 12(a). However, the sequence length averages for 4-acetoxystyrene exhibit only a slight increase (1.19–1.75 and 1.37–2.64 for number and weight averages, respectively) accompanied by a small increase in the SDI (1.17–1.51) as shown in Figure 12(b). Compared to styrene, 4-acetoxystyrene is continually incorporated in very short segments over the course of the entire polymerisation. Additionally, the polydispersity remains low throughout the course of the polymerisation indicating a high degree of uniformity of chain lengths. Although the amount of 4-acetoxystyrene increases over the course of the polymerisation, it is only incorporated in very short segments between longer homologous segments of styrene.

Another useful measure of the monomer arrangement of the copolymer is the determination of SLD, which describes the fraction of homologous sequence lengths of each monomer. The overall number and weight average SLDs for styrene and 4-acetoxystyrene are shown in Figure 13 for the final polymer in the reactor at 4 h. For both monomers, nearly the entire number fraction

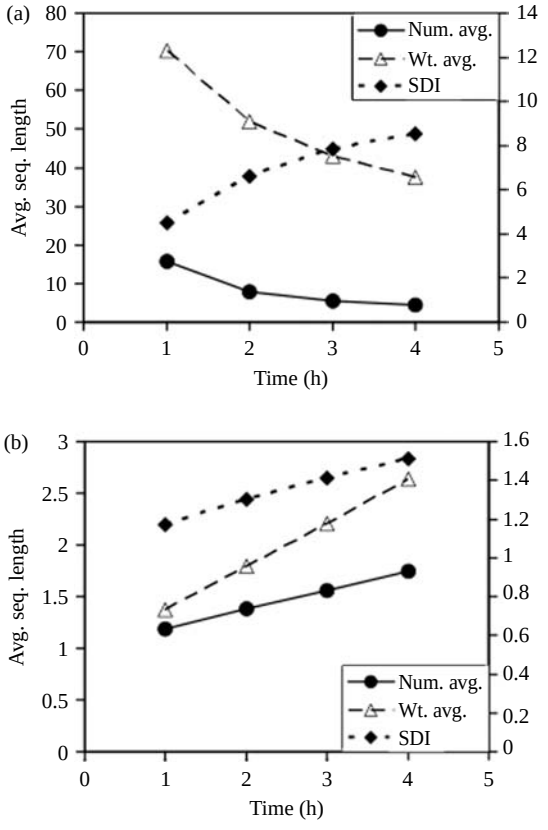

Figure 12. Average sequence lengths and SLD index (SDI; right *y*-axis) for macroinitiated gradient copolymer for (a) styrene and (b) 4-acetoxystyrene.

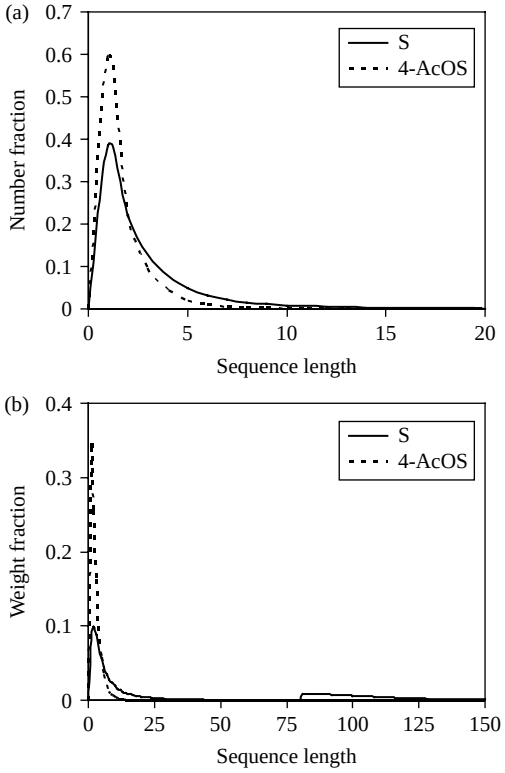

Figure 13. (a) Number and (b) weight fraction SLDs for macroinitiated gradient copolymer at a reaction time of 4 h.

distribution of chains is contained within segment lengths of 20 and less, with the styrene segments longer in average length as determined by the number of average sequence lengths as shown in Figure 13(a). It is also notable that there is no significant peak at the macroinitiator length ($DP_n = 81$) as would be expected. Figure 13(b) shows the weight fraction SLD; similar to the number fraction distribution, both monomers exist in short segment lengths with styrene exhibiting a tail originating from the macroinitiator. Similarly, 4-acetoxystyrene sequences are concentrated at very short lengths consistent with the sequence length averages.

Based on this distribution, it is apparent that the majority of sequences of both monomers are mostly of short length. Based on these observations from the triad and sequence length data, it is evident that the simulated gradient copolymer only possesses a weak composition gradient. The copolymer possesses an overall styrene fraction of 0.72 at the conclusion of the polymerisation, indicating that it is predominantly styrene, which is consistent with the triad distributions and number average sequence lengths. For all chain fractions, including the capped chains that are continuously initiated, the predominant triad is the all styrene (000) triad, indicating that all fractions possess a high number of styrene units in sequence. Over the course of the polymerisation, the number of triads containing 4-acetoxystyrene increases, but never to a significant extent. This is also consistent with the number average sequence length of styrene for each chain fraction. While for all chain fractions the number average sequence length of styrene decreases significantly, the number average sequence length of 4-acetoxystyrene only undergoes a slight increase. Although the fraction of triads containing 4-acetoxystyrene increases over the course of the polymerisation, the shift in the distribution indicates that 4-acetoxystyrene is not incorporated to a significant extent. The all 4-acetoxystyrene triad (111) is present in very low amounts in all chain fractions, indicating that the monomer does not get incorporated as homopolymer segments at the tail end of the copolymer. This is also consistent with the number average sequence lengths for the chain fractions as the number average sequence length for styrene decreases dramatically, but the corresponding average for 4-acetoxystyrene only increases slightly and remains quite low reaching a final value of 1.75. For a fully tapered, symmetric gradient copolymer, it would be expected that the two number average sequence lengths would be relatively close at the conclusion of the polymerisation. However, since the fractions of the monomers at the end of the copolymerisation in the batch are nearly equal, the 4-acetoxystyrene cannot be incorporated in significant amounts as it is never the dominant monomer in the reaction charge.

A second gradient copolymer synthesis was simulated using another set of experimental conditions studied by Kim et al. [7]. This synthesis was aimed at increasing the amount of 4-acetoxystyrene in the copolymer. The initial mole ratio of styrene/4-acetoxystyrene was 4:1 with an increased flow rate of 0.07 ml/min. After 3 h, the simulation predicts a styrene batch fraction of 0.41 with a styrene copolymer fraction of 0.63 with a number average degree of polymerisation of 299. The cumulative styrene fraction as a function of the normalised length of the chain is shown in Figure 14; similar to Figure 4, the simulation provides reasonable agreement with experimental data at the beginning of the chain and has a moderate overshoot at the tail end. The CCD of the macroinitiated capped chains for this case is shown in Figure S1 of the Supplementary Information which is similar to the previous case, as the asymmetry of the lobe indicates the change in composition. The triad distributions as a function of time are shown in Figure S2 of the Supplementary Information, indicating a significant shift from styrene-dominated triads to 4-acetoxystyrene-dominated triads. As shown in Figure S3 of the Supplementary Information, the number and weight average sequence lengths for styrene decrease with time while the number and weight average sequence lengths for 4-acetoxystyrene increase. The overall SLDs are shown in Figure S4 of the Supplementary Information. Both the number and weight fraction distributions show a high degree of similarity between styrene and 4-acetoxystyrene at low sequence lengths, with the weight fraction distribution indicating a larger fraction of longer styrene sequences originating from the macroinitiator. While the

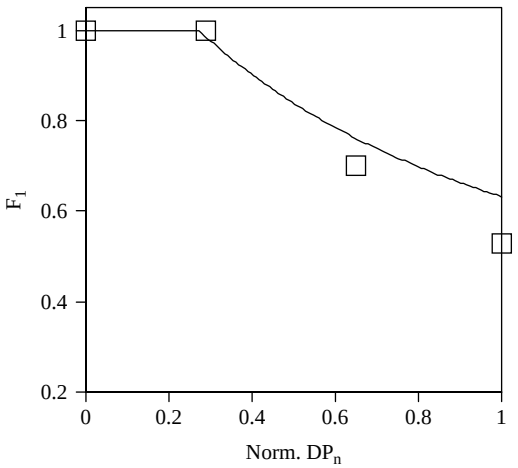

Figure 14. Cumulative styrene fraction as a function of normalised chain length for gradient copolymer synthesis with mixed initial batch (4:1 styrene to 4-acetoxystyrene) and increased flow rate (0.07 ml/min compared to 0.05 ml/min). The line represents the simulation results and experimental data of Kim et al. [7] is shown by the open symbols.

triad distributions show higher fractions of 4-acetoxystyrene-rich triads compared to the previous case, the final number average sequence lengths are comparable to those for the previous case shown in Figure 12. However, the number average sequence length for styrene declines significantly less compared to the copolymer synthesised using an all-styrene initial batch, indicating a lower degree of tapering. For both cases, it can be inferred that the copolymer backbone consists entirely of oligomeric sequence lengths with no significant amount of lengthy homologous sequences of 4-acetoxystyrene at the tail ends of chains.

It is evident based on the simulation data that while the polymerisation systems manage to incorporate a significant degree of styrene at the head end of the chains, the copolymers appear to taper but do not always contain a significant amount of 4-acetoxystyrene towards the ends of these chains. In all cases, the average sequence length for 4-acetoxystyrene is short, even when the tail ends are rich in 4-acetoxystyrene. Several factors determine the shape of the compositional gradient including monomer reactivity ratios, initial batch charge, semi-batch flow rate and conversion level. To explore the effect of these factors individually, we utilised KMC simulations to examine the effect of adjusting experimental parameters on the compositional gradient. Although it has been shown that reactivity ratios play a significant role in the gradient character of batch copolymerisation, we examined the styrene/4-acetoxystyrene system in detail and focused on altering the amount of 4-acetoxystyrene in the reaction through increases in flow rate and initial charge for the same reaction time. An increase in the ratio of 4-acetoxystyrene to styrene in the reacting batch will allow for a higher mole fraction of the monomer within the copolymer, but the degree to which the gradient shape is affected is of particular interest.

The first scenario that was modelled was to increase the initial composition in the batch. As opposed to the initial charge consisting entirely of styrene, an 80:20 styrene-to-4-acetoxystyrene ratio was used in the initial batch. This is the same composition as was used in the second macroinitiated system discussed above, but for that system, two changes, i.e. initial batch composition and flow rate, were made simultaneously. Simulations in which one variable is changed at a time will allow the effects of these two variables to be deconvoluted. The CCD of the macroinitiated capped chains for the final copolymer is shown in Figure 15(a) and the triad distribution is shown in Figure 16(a). As indicated by the more dramatic decrease in the slope of the lobe as a function of DP_n compared to the macroinitiated copolymer with an all-styrene initial batch shown in Figure 9(a), a higher degree of 4-acetoxystyrene is incorporated into the copolymer with a final styrene mole fraction of 0.66 in the copolymer with a batch composition of 0.44. This copolymer composition is lower than the all-styrene batch case of 0.78 at 3 h and close to the mixed batch composition of 0.63. The DP_n of the copolymer is 293, significantly lower than the all-styrene batch case DP_n of 425 but close to the mixed batch case DP_n of 299. As shown by the triad distribution, 4-acetoxystyrene incorporation is improved moderately as manifested in the decrease in 000 triads and increase in 4-acetoxystyrene-rich triads compared to the all-styrene batch case for 3 h shown in Figure 11(c). The number average sequence lengths are 3.83 and 1.96 for styrene and 4-acetoxystyrene, respectively, similar to the values obtained from the macroinitiated copolymer with mixed initial batch fraction. The number and weight fraction SLDs are shown in Figure S5 of the Supplementary Information. These distributions are relatively similar to the macroinitiated gradient copolymer with a mixed initial batch fraction shown in Figure S4 of the Supplementary Information. Both the number and weight fraction SLDs indicate the predominance of segment lengths <10 for both styrene and 4-acetoxystyrene with the weight fraction indicating the presence of longer sequence lengths originating from the macroinitiator.

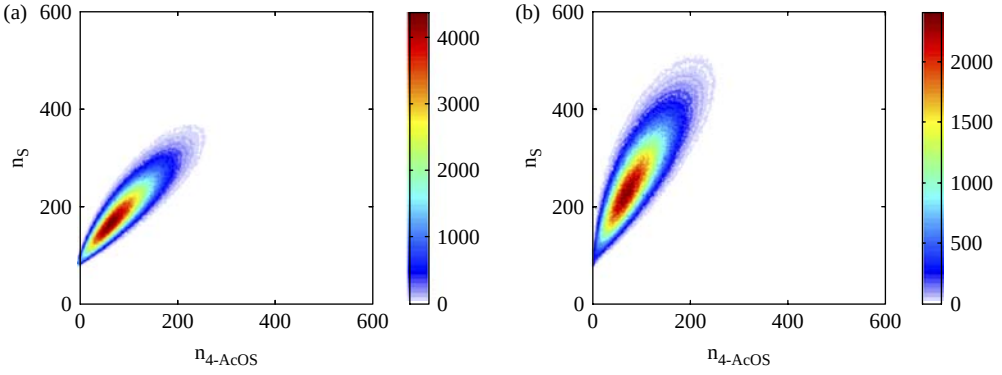

Figure 15. CCD plots of macroinitiated capped chains for gradient copolymerisation with (a) increased 4-acetoxystyrene initial batch composition (4:1 ratio) after 3 h and (b) increased flow rate (0.07 ml/min) after 3 h.

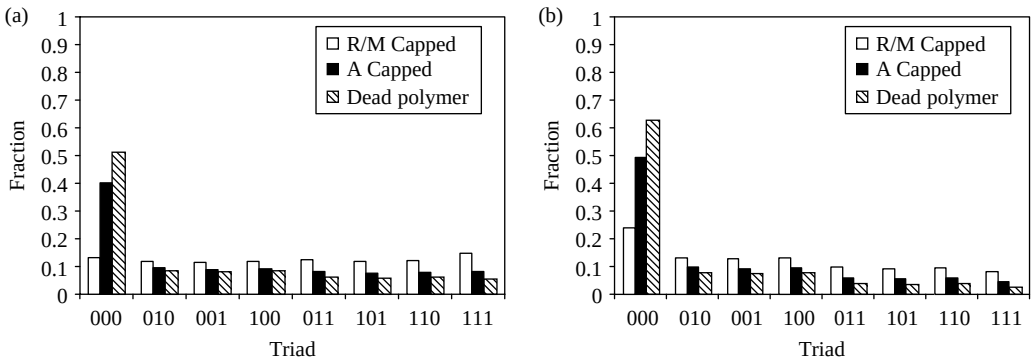

Figure 16. Triad distributions for gradient copolymerisation with (a) increased 4-acetoxystyrene initial batch composition (4:1 ratio) after 3 h and (b) increased flow rate (0.07 ml/min) after 3 h.

Next, an increase in the 4-acetoxystyrene flow rate to the system was assessed using KMC simulations. The flow rate was increased from 0.05 to 0.07 ml/min, with all other reaction conditions held at their original values, to introduce more 4-acetoxystyrene over the same reaction time. As shown by the CCD for the macroinitiated capped chains in Figure 15(b), the increase in flow rate has little effect on the copolymer, as the dominant lobe is similar in size and shape to that reported for the original conditions at 3 h shown in Figure 9(d). The styrene fractions in the copolymer and batch were determined to be 74 and 52%, respectively, compared to a copolymer fraction of 78% and batch fraction of 56% for the all-styrene batch case at 3 h of polymerisation. Similarly, the triad distribution in Figure 16(b) is not significantly different from that of the original case after 3 h shown in Figure 11(c). The number average sequence lengths are relatively similar to the all-styrene batch case at 3 h with values of 4.79 and 1.68 for styrene and 4-acetoxystyrene, respectively. The number average degree of polymerisation was 347, which is close to the all-styrene batch case value of 345. The number and weight fraction SLDs are shown in Figure S6 of the Supplementary Information. Compared to the previous case, the styrene SLDs possess more longer homologous segments of styrene, while 4-acetoxystyrene segments are predominantly <5 in length, indicating that this increase in flow rate had a weaker effect. It is clear from these results that a more dramatic increase in the flow rate would have to be instituted to have a marked effect on the backbone monomer arrangement. In addition, these simulations reveal that altering the initial batch composition was the dominant effect when the sequence characteristics of the two macroinitiated copolymers were compared.

Next, we sought to examine the effect of extreme changes in reaction conditions on the chain sequence characteristics. While it is apparent that increasing conversion is effective in incorporating significant amounts of comonomer into chains, a concomitant increase in the number average degree of polymerisation is observed. Significant increases in the batch composition and flow rate are capable of introducing larger amounts of 4-acetoxystyrene in the reaction mixture without requiring an increase in reaction time and a subsequent increase in chain length. The first case examined was to increase the initial batch composition to an equimolar mixture of

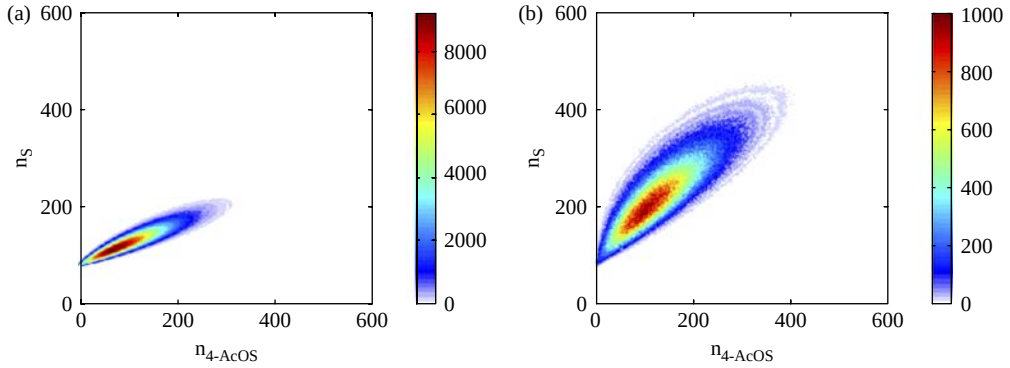

Figure 17. CCD plots of macroinitiated capped chains for copolymer synthesised for 3 h with (a) 50/50 styrene/4-acetoxystyrene initial batch composition and (b) increased 4-acetoxystyrene flow rate of 0.15 ml/min.

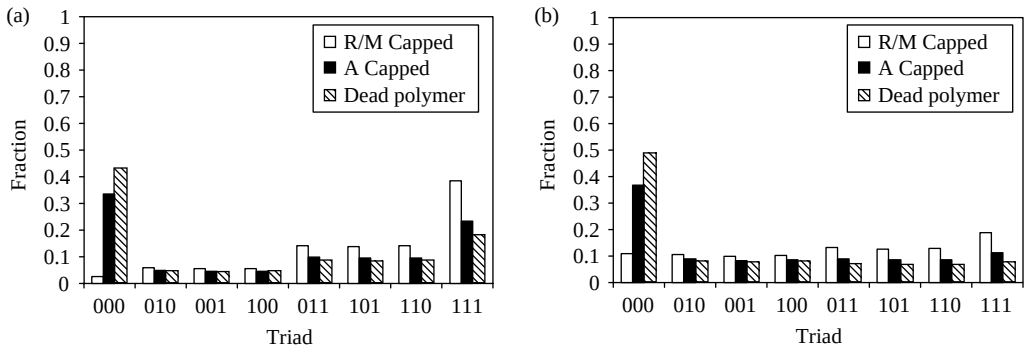

Figure 18. Triad distributions for macroinitiated copolymer polymerised for 3 h with (a) 50/50 styrene/4-acetoxystyrene initial batch composition and (b) increased 4-acetoxystyrene flow rate of 0.15 ml/min.

styrene and 4-acetoxystyrene. The CCD of the macroinitiated capped chains for this case is shown in Figure 17(a). The slope of the plot indicates that a significant amount of 4-acetoxystyrene was polymerised. However, the styrene fraction in the copolymer is 52% with a batch fraction of 27%, and the chains possess a DP_n of 249, indicating that the macroinitiator is a significant fraction of the chain length. The styrene fractions and DP_n are significantly lower compared to the 3 h all-styrene batch case values of 55% styrene batch fraction and 78% styrene copolymer fraction with a DP_n of 345. The triad fractions are shown in Figure 18(a) and indicate an abundance of 4-acetoxystyrene-rich triads. The number average sequence lengths were 3.61 and 3.29 for styrene and 4-acetoxystyrene, respectively, with the SLDs indicating longer homologous segments of 4-acetoxystyrene as shown in Figure S7 of the Supplementary Information. Although it is apparent that a significant amount of 4-acetoxystyrene gets incorporated into the tail end of the chain, the majority of the styrene fraction exists as the macroinitiator block, which implies there is little tapering from the head ends of the chains.

The next scenario examined was to incorporate a significantly larger flow rate to incorporate more 4-acetoxystyrene into the reactor during the given reaction time. For the analysis, the flow rate was tripled to 0.15 ml/min using an all-styrene initial batch with the other reaction conditions fixed at the base case values. The CCD of the macroinitiated capped chains for this case is shown in Figure 17(b) and reveals a larger, asymmetric lobe, indicating longer chain lengths and a more dramatic compositional gradient. The styrene fraction in the copolymer was determined as 62% with a batch fraction of 40%, and the number average degree of polymerisation was 363. Compared to the previous test case, the styrene fractions are significantly lower without a significant decrease in the DP_n. The triad distribution is shown in Figure 18(b) indicating a predominance of the 000 triad with relatively balanced amounts of the remaining triads. The number average sequence lengths were determined to be 3.57 and 2.16 for styrene and 4-acetoxystyrene, respectively. The SLD is shown in Figure S8 of the Supplementary Information and indicates relatively symmetric sequences for both comonomers. While the number average sequence lengths are relatively close to the averages for the macroinitiated copolymer synthesised using a mixed initial batch fraction, the head end is fully tapered as the initial batch contains all styrene. Although incorporation of 4-acetoxystyrene is increased, the tail end is not completely tapered in the sense that it is not composed of long, homologous sequences of 4-acetoxystyrene.

4. Conclusions

Utilising a mechanistic approach, explicit stochastic simulations were carried out to describe copolymerisation systems using a KMC algorithm. Because these simulations track chains explicitly rather than using composite values like most continuum models, microscopic features of the copolymeric systems can be captured. By utilising explicit modelling for NM-CRP gradient copolymerisation, methodologies were developed that are capable of describing these systems at a highly detailed level.

Initial models focused on the simulation of the CCD for copolymer systems. The CCD offers a visual description combining the size and composition distributions for a particular copolymer. Although explicit sequence data cannot be extracted from these plots, they give a qualitative assessment of the general structure of the copolymer, e.g. block, random, alternating, gradient, from the shape of the plot. The CCD also provides a concise visual description of the copolymer and its chain fractions.

A more explicit methodology was developed which tracked the entire sequence of copolymer chains in the system. By tracking individual chains as binary strings, the KMC simulations are able to provide triad distribution data as well as SLDs and average sequence lengths. We applied

this methodology to two styrene/4-acetoxystyrene gradient copolymer syntheses described in the literature. It was concluded that while each of these systems possessed compositional gradients, none of these copolymers was fully tapered from end to end. In all cases, the tail ends of the chains were never fully tapered into 4-acetoxystyrene homopolymer. While tapering was achieved at the head end through the use of the macroinitiator, the compositional gradient was not strong enough to fully convert the tail end into 4-acetoxystyrene homopolymer.

Test cases were run in which initial batch composition and flow rate were altered to determine their individual effects on the copolymer sequence characteristics. These cases indicated that more dramatic changes than those explored experimentally were required to induce larger changes in composition. Initial batch composition and flow rate were increased significantly. Although a large increase in 4-acetoxystyrene incorporation can be induced by using more 4-acetoxystyrene in the initial reaction mixture, tapering at the head end is lost and most of the styrene exists as a blocked end from the macroinitiator. A threefold increase in the flow rate was able to incorporate more 4-acetoxystyrene while maintaining tapering at the head end. However, tail end tapering was still not achieved. It is apparent from this analysis that it is difficult to induce tapering at both ends of the chains. One option would be to alter the flow rate over the course of the reaction which would allow tapering from the macroinitiated head end and convert the tail end into longer homologous segments of the second monomer. In order to tailor more refined compositional gradients, additional semi-batch studies must be pursued. Alteration of these gradients can be quantified using the current methodology and would enable further studies relating physical properties to chainwise composition.

Acknowledgements

This work was supported by the MRSEC programme of the National Science Foundation (DMR-0076097 and DMR-0520513) at the Materials Research Center of Northwestern University.

References

[1] C.J. Hawker, A.W. Bosman, and E. Harth, *New polymer synthesis by nitroxide mediated living radical polymerizations*, Chem. Rev. 101 (2001), pp. 3661–3688.

[2] S.L. Rosen, *Fundamental Principles of Polymeric Materials*, Wiley, New York, NY, 1993.

[3] U. Beginn, *Gradient copolymers*, Coll. Polym. Sci. 286 (13) (2008), pp. 1465–1474.

[4] B. Klumperman, *Statistical, alternating, and gradient copolymers*, Macromol. Eng. 2 (2007), pp. 813–838.

[5] J. Kim, M.K. Gray, H. Zhou, S.T. Nguyen, and J.M. Torkelson, *Polymer blend compatibilization by gradient copolymer addition during melt processing: Stabilization of dispersed phase to static coarsening*, Macromolecules 38 (4) (2005), pp. 1037–1040.

[6] J. Kim, R.W. Sandoval, C.M. Dettmer, S.T. Nguyen, and J.M. Torkelson, *Compatibilized polymer blends with nanoscale or sub-micron dispersed phases achieved by hydrogen-bonding effects: Block copolymer vs. blocky gradient copolymer addition*, Polymer 49 (11) (2008), pp. 2686–2697.

[7] J. Kim, H. Zhou, S.T. Nguyen, and J.M. Torkelson, *Synthesis and application of styrene/4-hydroxystyrene gradient copolymers made by controlled radical polymerization: Compatibilization of immiscible polymer blends via hydrogen-bonding effects*, Polymer 47 (16) (2006), pp. 5799–5809.

[8] M.M. Mok, J. Kim, and J.M. Torkelson, *Gradient copolymers with broad glass transition temperature regions: Design of purely interphase compositions for damping applications*, J. Polym. Sci. B: Polym. Phys. 46 (1) (2007), pp. 48–58.

[9] M.M. Mok, S. Pujari, W.R. Burghardt, C.M. Dettmer, S.T. Nguyen, C.J. Ellison, and J.M. Torkelson, *Microphase separation and shear alignment of gradient copolymers: Melt rheology and small-angle X-ray scattering analysis*, Macromolecules 41 (15) (2008), pp. 5818–5829.

[10] M. Kryszewski, *Gradient polymers and copolymers*, Polym. Adv. Tech. 9 (1998), pp. 244–259.

[11] K. Matyjaszewski, M.J. Ziegler, S.V. Arehart, D. Greszta, and T. Pakula, *Gradient copolymers by atom transfer radical copolymerization*, J. Phys. Org. Chem. 13 (2000), pp. 775–786.

[12] E. Rizzardo, J. Chiefari, B.Y.K. Chong, F. Ercole, J. Krstina, J. Jeffery, T.P.T. Le, R.T.A. Mayadunne, G.F. Meijs, C.L. Moad, G. Moad, and S.H. Thang, *Tailored polymers by free radical processes*, Macromol. Symp. 143 (1999), pp. 291–307.

[13] K. Karaky, E. Pere, C. Pouchan, J. Desbrieres, C. Derail, and L. Billon, *Effect of the synthetic methodology on molecular architecture: From statistical to gradient copolymers*, Soft Matter 2 (2006), pp. 770–778.

[14] M.K. Gray, H.Y. Zhou, S.T. Nguyen, and J.M. Torkelson, *Synthesis and glass transition behavior of high molecular weight styrene/4-acetoxystyrene and styrene/4-hydroxystyrene gradient copolymers made via nitroxide-mediated controlled radical polymerization*, Macromolecules 37 (2004), pp. 5586–5595.

[15] R. Wang, Y. Luo, B. Li, and S. Zhu, *Control of gradient copolymer composition in ATRP using semibatch feeding policy*, AIChE J. 53 (1) (2007), pp. 174–186.

[16] J.C. Randall, *Polymer sequence determination: Carbon-13 NMR method*, Academic Press, New York, NY, 1977.

[17] J.J. Semler, Y.K. Jhon, A. Tonelli, M. Beevers, R. Krishnamoorti, and J. Genzer, *Facile method of controlling monomer sequence distributions in random copolymers*, Adv. Mater. 19 (19) (2007), pp. 2877–2883.

[18] A.E. Tonelli, *A case for characterizing polymers with the Kerr effect*, Macromolecules 42 (12) (2009), pp. 3830–3840.

[19] R.Y. Tabash and F. Teymour, *Analyzing compositional drift transients in copolymerization systems using digital encoding*, Chem. Eng. Sci. 59 (2004), pp. 5129–5137.

[20] R.Y. Tabash, F. Teymour, and J.A. Debling, *Modeling linear free radical copolymerization by digital encoding*, Macromolecules 39 (2006), pp. 829–843.

[21] J.A. Debling and F. Teymour, *A new arithmetic for linear free radical copolymerization*, Macromol. Symp. 182 (2002), pp. 195–207.

[22] Y. Shi, F. Qiu, Q. Meng, and Y. Zhang, *Monte Carlo simulation on sequence statistical structures of gradient copolymers*, e-Polymers 115 (2008), pp. 1–16.

[23] R.X.E. Willemse and A.M. Van Herk, *Copolymerization kinetics of methyl methacrylate–styrene obtained by PLP-MALDI-ToF-MS*, J. Am. Chem. Soc. 128 (2006), pp. 4471–4480.

[24] R.X.E. Willemse, B.B.P. Staal, E.H.D. Donkers, and A.M. Van Herk, *Copolymer fingerprints of polystyrene-block-polyisoprene by MALDI-ToF-MS*, Macromolecules 37 (2004), pp. 5717–5723.

[25] R.X.E. Willemse, *New Insights into Free-Radical (Co)Polymerization Kinetics*, Technische Universiteit Eindhoven, Eindhoven, The Netherlands, 2005.

[26] W.H. Stockmayer, *Distribution of chain lengths and compositions in copolymers*, J. Chem. Phys. 13 (1945), pp. 199–207.

[27] S. Anantawaraskul, J.B.P. Soares, and P.M. Wood-Adams, *Chemical composition distribution of multicomponent copolymers*, Macromol. Theory Simul. 12 (2003), pp. 229–236.

[28] S. Costeux, S. Anantawaraskul, P.M. Wood-Adams, and J.B.P. Soares, *Distribution of the longest ethylene sequence in ethylene/α-olefin copolymers synthesized with single-site-type catalysts*, Macromol. Theory Simul. 11 (2002), pp. 326–341.

[29] M.A. Al-Saleh and L.C. Simon, *Monte Carlo simulation of ethylene copolymers: A look into the monomer sequence distribution*, Macromol. Symp. 243 (2006), pp. 123–131.

[30] T.M. Kruse, R. Souleimanova, A. Cho, M.K. Gray, J.M. Torkelson, and L.J. Broadbelt, *Limitations in the synthesis of high molecular weight polymers via nitroxide-mediated controlled radical polymerization: Modeling studies*, Macromolecules 36 (20) (2003), pp. 7812–7823.

[31] N. Li, A.S. Cho, L.J. Broadbelt, and R.A. Hutchinson, *Low conversion 4-acetoxystyrene free-radical polymerization kinetics determined by pulsed-laser and thermal polymerization*, Macromol. Chem. Phys. 207 (2006), pp. 1429–1438.

[32] J.M. Catala, F. Bubel, and S.O. Hammouch, *Living radical polymerization: Kinetic results*, Macromolecules 28 (24) (1995), pp. 8441–8443.

[33] M.K. Gray, H.Y. Zhou, S.T. Nguyen, and J.M. Torkelson, *Limitations in the synthesis of high molecular weight polymers via nitroxide-mediated controlled radical polymerization: Experimental studies*, Macromolecules 36 (2003), pp. 5792–5797.

[34] A.S. Cho, L. Wang, E. Dowuona, H. Zhou, S.T. Nguyen, and L.J. Broadbelt, *4-Acetoxystyrene nitroxide-mediated controlled radical polymerization: Comparison with styrene*, J. Appl. Polym. Sci. in press (2009).

[35] D. Woo, J. Kim, M.-H. Suh, H. Zhou, S.T. Nguyen, S.-H. Lee, and J.M. Torkelson, *Styrene/4-hydroxystyrene random, block and gradient copolymers modified with an organic dye: Synthesis by controlled radical polymerization and characterization of electrorheological properties*, Polymer 47 (2006), pp. 3287–3291.

[36] G.G. Barclay, C.J. Hawker, H. Ito, A. Orellana, P.R.L. Malenfant, and R.F. Sinta, *The 'living' free radical synthesis of poly (4-hydroxystyrene): Physical properties and dissolution behavior*, Macromolecules 31 (1998), pp. 1024–1031.

[37] J.M. Nasrullah, S. Raja, K. Vijayakumaran, and R. Dhamodharan, *A practical route for the preparation of poly(4-hydroxystyrene), a useful photoresist material*, J. Polym. Sci. A: Polym. Chem. 38 (2000), pp. 453–461.

[38] F.R. Mayo and F.M. Lewis, *Copolymerization. I. A basis for comparing the behavior of monomers in copolymerization; The copolymerization of styrene and methyl methacrylate*, J. Am. Chem. Soc. 66 (1944), pp. 1594–1601.

[39] D. Braun, W. Czerwinski, G. Disselhoff, F. Tudos, T. Kelen, and B. Turcsanyi, *Analysis of the linear methods for determining copolymerization reactivity ratios. 7. A critical reexamination of radical copolymerizations of styrene*, Angew. Makromol. Chem. 125 (1984), pp. 161–205.

[40] T. Fukuda, Y.-D. Ma, and H. Inagaki, *Free-radical copolymerization. 6: New interpretation for the propagation rate versus composition curve*, Makromol. Chem., Rapid Commun. 8 (1987), pp. 495–499.

[41] M.C. Piton, M.A. Winnik, T.P. Davis, and K.F. O'Driscoll, *Copolymerization kinetics of 4-methoxystyrene with methyl methacrylate and 4-methoxystyrene with styrene: A test of the penultimate model*, J. Polym. Sci. A: Polym. Chem. 28 (1990), pp. 2097–2106.

[42] D.T. Gillespie, *A general method for numerically solving the stochastic time evolution of coupled chemical reactions*, J. Comp. Sci. 22 (1976), pp. 403–434.

[43] D.T. Gillespie, *Exact stochastic simulation of coupled chemical reactions*, J. Phys. Chem. 81 (25) (1977), pp. 2340–2361.

[44] S. Huijser, B.B.P. Staal, J. Huang, R. Duchateau, and C.E. Koning, *Chemical composition and topology of poly(lactide-co-glycolide) revealed by pushing MALD-ToF-MS to its limit*, Angew. Chem., Int. Ed. 45 (2006), pp. 4104–4108.

[45] B.B.P. Staal, *Characterization of (co)polymers by MALDI-ToF-MS*, Technische Universiteit Eindhoven, Eindhoven, The Netherlands, 2005.

[46] L. Wang and L.J. Broadbelt, *Kinetics of segment formation in nitroxide-mediated controlled radical polymerization: Comparison with classic theory*, Macromolecules, submitted (2009).

[47] A. Goto and T. Fukuda, *Comparative studies on activation rate constants for some styrene/nitroxide systems*, Macromol. Chem. Phys. 201 (2000), pp. 2138–2142.

[48] D. Greszta and K. Matyjaszewski, *Mechanism of controlled/'living' radical polymerization of styrene in the presence of nitroxyl radicals. Kinetics and simulations*, Macromolecules 29 (1996), pp. 7661–7670.

[49] M. Buback and F.-D. Kuchta, *Termination kinetics of free-radical polymerization of styrene over an extended temperature and pressure range*, Macromol. Chem. Phys. 198 (1997), pp. 1455–1480.

[50] M. Buback, R.G. Gilbert, R.A. Hutchinson, B. Klumperman, F.-D. Kuchta, B.G. Manders, K.F. O'driscoll, G.T. Russell, and J. Schweer, *Critically evaluated rate coefficients for free-radical polymerization*, Macromol. Chem. Phys. 196 (1995), pp. 3267–3280.

[51] J.D. Campbell, F. Teymour, and M. Morbidelli, *High temperature free radical polymerization. 1. Investigation of continuous styrene polymerization*, Macromolecules 36 (2003), pp. 5491–5501.

[52] A.W. Hui and A.E. Hamielec, *Thermal polymerization of styrene at high conversions and temperatures. An experimental study*, J. Appl. Polym. Sci. 16 (1972), pp. 749–769.